SSS-R-78-3618

FE-1770-41
Distribution Category UC-90c

COMPUTER MODELING OF COAL GASIFICATION REACTORS

Quarterly Technical Progress Report
For the Period October 1, 1977 - December 31, 1977

Thomas R. Blake

Systems, Science and Software
P. O. Box 1620
La Jolla, California 92038

January 1978

PREPARED FOR THE UNITED STATES
DEPARTMENT OF ENERGY

Under Contract No. EX-76-C-01-1770

TABLE OF CONTENTS

ABSTRACT

This report presents a summary of the work accomplished during the tenth quarter of a three year study conducted for the U. S. Department of Energy, under Contract No. E(49-18)-1770, to develop and apply computer codes simulating the performance of fluidized bed and entrained flow coal gasification reactors.

SECTION I

OBJECTIVE AND SCOPE OF WORK

The purpose of this three year program is to develop and apply general computer models that will expedite the development and aid in the optimization and scale-up of reactors for coal gasification. Initial applications will be to fluidized bed gasification processes; subsequently both entrained flow reactors and fast fluidized beds will be examined.

During the first year (Year 1), work will be initiated on the fluidized bed model in the areas of multiphase fluid flow without chemical reactions, and chemical reactions without fluid flow. The models, developed to represent these aspects of gasification processes, will be combined in the second year (Year 2) of the program into a numerical model of a time-dependent field description of fluidized bed flows in two space dimensions. Calculations will be performed with the prototype code during Years 1 and 2 to verify the accuracy of the formulations employed. In Year 2, these calculations should provide some preliminary results relevant to coal gasification.

During Year 2, a computer model for entrained flow gasifiers will be formulated and the coal chemistry defined; this model will provide a field description of entrained flows in two and three spatial dimensions. Nonreactive flow calculations will be performed for entrained flow processes by the end of Year 2.

In the third year (Year 3) of the program, application of the fluidized bed computer model to specific gasifier processes will be extended and a model which includes three-dimensional effects developed. Also, during this third year the coal chemistry defined in Year 2 will be combined with the entrained flow computer model and some calculations of such gasifier configurations performed.

SECTION II

SUMMARY OF PROGRESS TO DATE

The development of the computer model for fluidized bed coal gasification reactors was continued. This model can now represent both planar and axisymmetric geometries; the development and testing of this axisymmetric capability was completed. Comparisons between numerical simulations of axisymmetric jets and bubbles and the corresponding data show excellent agreement. A new formulation for the numerical simulation of the convective transport of gas species and temperature was developed and is being incorporated into the computer model.

Calculations of jet penetration and bubble formation, with application to the Synthane gasifier were performed. These studies were directed to the prediction of bed height and mass flow influences upon bubble formation and rise in the vicinity of the Synthane distributor plate.

A three dimensional version of the entrained flow coal gasification computer model was developed and preliminary calculations were performed.

The entrained flow model was also used to calculate two dimensional channel flows of a particle laden gas. Comparisons between these calculations and exact solutions showed excellent agreement.

Theoretical studies of the heterogeneous and homogeneous reactions appropriate to coal gasification reactors were continued. A single particle model for coal/char devolatilization was developed to describe species and total volatile yield in entrained flow coal gasification; this model utilizes the kinetic data of Howard and his coworkers. A study of burning carbon particles, including transient heating, particle porosity and homogeneous reactions was completed; comparisons of predicted burnout time with data show good qualitative and quantitative agreement.

SECTION III

DETAILED DESCRIPTION OF TECHNICAL PROGRESS

3.1 TASK 00: MANAGEMENT, DOCUMENTATION AND CONSULTING

A draft copy of our annual report, "Computer Modeling of Coal Gasification Reactors, Year 2", was submitted to DOE for review.

Potential applications of the fluidized bed and entrained flow codes were discussed with staff members of EPRI (October 5), Bechtel (October 5) and Lockheed (October 27). In the latter meeting the nature of the Lockheed pulverized coal feeder and the gas-solid particle dynamics were examined. It appears that the entrained flow code could be quite useful in a study of that coal feeding process and, in particular, to examine the scale-up of the design.

Dr. Blake attended the Ninth Synthetic Pipeline Gas Symposium in Chicago on October 31 through November 2 and the American Institute of Chemical Engineers Annual Meeting in New York on November 14 through 16.

Drs. Blake and Henline visited Professor Jack Howard at the Massachusetts Institute of Technology and Dr. Shivadev Ubhayaker at AVCO, Everett on November 3-4 to discuss analytical models and experimental data on coal/char devolatilization. The research of Professor Howard and his colleagues, wherein the kinetics of species and total volatile yield is described by a distribution of activation energies, is being used in the Systems, Science and Software (S^3) modeling of devolatilization for entrained flow coal gasification.

Dr. Schneyer presented a paper, "A Numerical Simulation Model for Entrained Flow Coal Gasification, I. The Hydrodynamical Model", (c.f., Blake, et al. [1978]) at the Miami International Conference on Alternative Energy Sources, December 5-7. The paper will be published in the conference proceedings (McGraw Hill). A sequel to this paper, including calculations of reactive flows typical of entrained flow combustion and gasification, "A Numerical Model of Coal Gasification in Entrained Flow Reactors", has since been accepted for presentation at the 71st Annual AIChE Meeting in 1978 [Schneyer, et al., 1978].

Dr. Blake visited DOE on December 20, and met with E. Clark, L. Naphtali and M. Carrington. He reviewed the status of the technical work and discussed (with M. Carrington) the

application of the S^3 model to the Westinghouse gasifier configuration.

Professor C. Y. Wen of West Virginia University continued his consulting activities in the area of the chemistry of steam-oxygen gasification. In addition, he is the principal investigator of a subcontract to West Virginia University for the development of a two phase model of fluidization for steam-oxygen gasification.

Professor Paul Libby of the University of California, San Diego, continued his studies of the heterogeneous and homogeneous reactions and transport processes associated with the oxidation of carbon particles.

Professor Joseph Yerushalmi consulted in the area of jet penetration and bubble formation in fluidized beds. He has contributed to an S^3 summary and review of existing theories, correlations and data on the subject of jets and fluidization.

3.2 TASK 01: FLUIDIZED BED COAL GASIFICATION MODEL

The development and modification of the fluidized bed coal gasification computer model was continued. A version of that code, designed to represent fluidized bed flows with axisymmetric geometries, was developed in the previous quarter [Blake, 1977]. That development and the numerical testing of this axisymmetric model was completed during the present quarter. The nature of the numerical model is essentially the same as that of the planar version of the code except that the convection of mass, momentum and energy and the specific character of the constitutive formulations now include the influences of cylindrical geometry. In addition, the Lagrangian representation of solid particle motion was modified to account for such geometric influences. This code will be applied in calculations of the detailed, quasi-axisymmetric flows from discrete orifices in fluidized bed distributor plates. The local influences of jets and bubbles from adjacent orifices will occur naturally in the calculation through the application of appropriate boundary conditions. Further, the intersection of the jet with adjacent jets and bubbles can be represented through a numerical mapping of the reactor field into a larger calculational grid, encompassing all of the orifices.

This axisymmetric fluidized bed model has been used to calculate jet penetration and bubble formation at a discrete orifice and the calculations have been compared with both theory and experiment. There is excellent agreement

between the numerical predictions and theoretical and experimental results on bubble size and rise velocity. A brief discussion of the axisymmetric model and some calculational results are presented in Appendix A of this report.

In addition to the numerical development associated with the axisymmetric code, we have elected to reformulate the numerical representation of convection of mass and energy in the fluidized bed model. At the present time (c.f., Blake, et al. [1977]) the calculation of gas species concentrations (density) and the local gas and solid phase temperature are performed simultaneously using implicit techniques. While this method of calculation provides the most complete description of the convection of mass and energy for the multicomponent gas and char flows in coal gasification reactors, it necessarily involves complicated and costly numerical algorithms and accounting procedures. For many fluidized regimes appropriate to coal gasification, we expect that an explicit calculation of this transport will be sufficiently accurate and will also permit dramatic reductions (likely a factor of 10 or greater) in computer time required for a given reactive flow calculation. This explicit treatment has been formulated and it will be included in the fluidized bed model during the next quarter. Again, the present implicit method is most general and will be used in those flow regimes where it is still required. Further, it will provide a necessary basis of comparison for this proposed explicit solution technique.

The application of the numerical model to simulate cold and hot flows in the Synthane reactor geometry was continued. In addition, theoretical studies of jet penetration and bubble formation were initiated; a review of existing data, correlations and theoretical models was completed. One objective of this combined numerical-theoretical study of the Synthane distributor plate flows is to investigate the applicability and scaling of cold flow visualization experiments to the hot reactive regime of the Synthane gasifier. Further, the examination of existing correlations such as discussed by Salvador and Keairns [1977a,b], together with the numerical simulation studies, provides a basis for interpretation and guidance for such cold flow studies. Specific numerical simulation studies of the Synthane reactor have included calculations for different bed heights (3-10 feet) with air fluidization of Synthane char at 40 atmospheres pressure and a superficial gas velocity of 0.5 ft/sec. We found that the jet formation and solid particle mixing at the orifice were not significantly influenced by the bed height. There was some solids convection at the distributor plate but the jet did not produce significant local bubbling. Our earlier calculations and theoretical studies have indicated that 40 atmosphere, ambient temperature air is an appropriate

fluid for scaling flow visualization tests to the hot, reactive, distributor plate flows in the Synthane gasifier.

A research group at West Virginia University (Principal Investigator, C. Y. Wen) is developing a classical two phase fluidization model of coal gasification reactors through a subcontract to Systems, Science and Software. This S^3/WVU model development was completed and sample calculations were performed. A documentation of this code is being prepared by WVU.

3.3 TASK 02: ENTRAINED FLOW COAL GASIFICATION MODEL

The development of the entrained flow coal gasification model was continued. In the previous quarter this finite element/finite difference computer code was generalized to treat transient flows in three spatial dimensions. That three dimensional version of the code was used in some preliminary and, therefore, brief calculations of the Foster Wheeler cold flow combustor stage configuration. The test problems verified the numerical algorithms defining the three dimensional finite element grid and provided preliminary tests of finite difference formulation of the three dimensional conservation equations.

In addition to the three dimensional calculations, some two dimensional simulations were performed. One of these studies provided a verification of the prediction of the coupled gas dynamics and solid particle motion through a comparison with an exact solution of such two phase flows. This comparison was with a steady, gas and particle, laminar Couette flow solution by Quan [1972]. In this problem the normal injection of spherical solid particles at a fixed rate from the lower wall, in a planar channel, and their non-normal absorption at the upper wall is added to the classical Couette flow. The solid particle-gas interaction provides a complex variation from the classical linear gas velocity profile. The numerical model was used to calculate the evolution of this flow to a final steady state and excellent agreement between this calculation and Quan's exact solution was obtained (c.f., Blake, Brownell and Schneyer [1978]). Again, this agreement provides an important verification of aspects of the entrained flow computer model. Of course, additional theoretical results and/or experimental data on turbulent reactive and nonreactive particle-gas flows are required to provide a complete verification of this code. We expect that the experimental work of, say, Smoot and his coworkers, e.g., Smoot and Hanks [1975] or Laurendau and his coworkers, e.g., Lenzer, et al. [1976] will, in the future, be useful in such verification studies.

The study of devolatilized coal/char was continued and a heterogeneous reaction model was formulated. This model is based upon the representation of a single particle wherein pyrolytic, polymerization and hydrogenation reactions occur within the particle and where intra and extra particle diffusive transport mechanisms influence the overall reaction rate. The kinetics models and physicochemical hypotheses of Howard and his coworkers (c.f., Anthony and Howard [1976] and Suuberg, et al. [1978]) are utilized. With this single particle model, a summation over many particles is then taken to derive the source (sink) terms representing interphase mass and energy exchange for the gas-particle flows. A discussion of this representation of devolatilization is presented in Appendix B.

The theoretical study of burning carbon particles (c.f., Blake [1977]) has been extended to include particle porosities and transient heating (and transient mass loss) of the carbon particles. In this analysis the important influences of Stefan flow and homogeneous chemistry upon the reaction rate control are delineated. Comparisons of predicated and experimental burnout times for oxidative environments have been made and these comparisons show excellent qualitative and quantitative agreement. In addition, the theoretical description provides insight into the mechanisms of particle mass loss and the details of the temperature and gas composition distribution, including flame front location, in the vicinity of the particle.

SECTION IV

CONCLUSIONS

In summary, we note the following aspects of our modeling effort.

- The fluidized bed computer model has been used in both planar and axisymmetric modes and comparisons between predictions and experiments on nonreactive flows show excellent agreement.

- The entrained flow computer model has been tested in limited three dimensional calculations.

APPENDIX A

FLUIDIZED BED COAL GASIFICATION MODEL IN CYLINDRICAL GEOMETRY

The fluidized bed coal gasification model has been extended to represent fluidization in cylindrical, axisymmetric configurations. This numerical model has the same basic formulation as that of the former planar version of the code [Blake, et al., 1976; Pritchett, et al., 1978] except that the convection of mass, momentum and energy and also the specific character of the constitutive formulations now include the influences of cylindrical geometry. In this appendix we present a brief description of the code and discuss some representative calculations with that numerical model.

A.1 GOVERNING EQUATIONS

The equations for the conservation of solid mass and gas species, the momentum equations of both the solid and gas phases and the total energy equation (c.f., Blake, et al. [1976]), together with constitutive equations, interaction functions and chemical kinetics provide the theoretical description of fluidized bed flows. These differential equations contain a number of terms which reflect the nature of the coordinate system. For the purposes of our present discussion, these equations are written below in cylindrical coordinates. The independent variables are y in vertical and r in radial directions and the corresponding velocity components are u_y, u_r for the solid and v_y, v_r for the gas.

Conservation of Solid Mass:

$$\frac{\partial}{\partial t}(\theta\rho_s) + \frac{\partial}{\partial y}(\theta\rho_s u_y) + \frac{1}{r}\frac{\partial}{\partial r}(r\theta\rho_s u_r) = -S \qquad (A.1)$$

Conservation of Gas Species:

$$\frac{\partial}{\partial t}\left[(1-\theta)\rho F_\alpha\right] + \frac{\partial}{\partial y}\left[(1-\theta)\rho F_\alpha v_y\right] + \frac{1}{r}\frac{\partial}{\partial r}\left[(1-\theta) r \rho F_\alpha v_r\right]$$

$$= S_\alpha + (1-\theta)\Omega_\alpha \qquad \alpha = 1,2\ldots,N \tag{A.2}$$

Conservation of Momentum for the Solid:

$$\frac{\partial}{\partial t}(\theta\rho_s u_y) + \frac{\partial}{\partial y}(\theta\rho_s u_y u_r) + \frac{1}{r}\frac{\partial}{\partial r}(r\theta\rho_s u_y^2) = -\theta\rho_s g$$

$$- \frac{\partial}{\partial y}(p_s + p) + \frac{\partial}{\partial y}\left[\bar{\lambda}_s\left\{\frac{\partial}{\partial y}u_y + \frac{1}{r}\frac{\partial}{\partial r}(ru_r)\right\}\right]$$

$$+ 2\frac{\partial}{\partial y}\left[\mu_s \frac{\partial}{\partial y}u_y\right] + \frac{1}{r}\frac{\partial}{\partial r}\left[r\mu_s\left(\frac{\partial}{\partial r}u_y + \frac{\partial}{\partial y}u_r\right)\right] \tag{A.3}$$

$$\frac{\partial}{\partial t}(\theta\rho_s u_r) + \frac{\partial}{\partial y}(\theta\rho_s u_y u_r) + \frac{1}{r}\frac{\partial}{\partial r}(r\theta\rho_s u_r^2) = -\frac{\partial}{\partial r}(p_s + p)$$

$$+ \frac{\partial}{\partial r}\left[\bar{\lambda}_s\left\{\frac{\partial}{\partial y}u_y + \frac{1}{r}\frac{\partial}{\partial r}(ru_r)\right\}\right] + \frac{2}{r}\frac{\partial}{\partial r}\left[r\mu_s\frac{\partial}{\partial r}u_r\right]$$

$$+ \frac{\partial}{\partial y}\left[\mu_s\left(\frac{\partial}{\partial y}u_r + \frac{\partial}{\partial r}u_y\right)\right] - 2\mu_s\frac{u_r}{r^2} \tag{A.4}$$

where p and p_s are the gas pressure and the solid pressure, μ_s is the shear viscosity coefficient for the solid and $\bar{\lambda}_s$ is defined in terms of the bulk, λ_s, and shear viscosities according to $\bar{\lambda}_s = \lambda_s - 2/3\ \mu_s$.

The solid pressure is defined as

$$p_s = \frac{a^2}{2}\rho_s^2(\theta-\theta_0)^2 \quad \text{for} \quad \theta > \theta_0$$

$$= 0 \quad \text{for} \quad \theta \leq \theta_0 \tag{A.5}$$

Conservation of Momentum for the Gas:

$$v_y = u_y - \frac{(1-\theta)}{B(\theta)} \frac{\partial}{\partial y} p \tag{A.6}$$

$$v_r = u_r - \frac{(1-\theta)}{B(\theta)} \frac{\partial}{\partial r} p \tag{A.7}$$

Conservation of Total Energy:

$$\begin{aligned}
&\frac{\partial}{\partial t} [(1-\theta)\ \rho e + \theta \rho_s e_s] + \frac{\partial}{\partial y} [(1-\theta)\ \rho e v_y + \theta \rho_s e_s u_y] \\
&\quad + \frac{1}{r} \frac{\partial}{\partial r} [r\ (1-\theta)\ \rho e v_r + r\theta \rho_s e_s u_r] = \frac{\partial}{\partial y} \left(\bar{K} \frac{\partial}{\partial y} T \right) \\
&\quad + \frac{1}{r} \frac{\partial}{\partial r} \left(r\bar{K} \frac{\partial}{\partial r} T \right) + \frac{\partial}{\partial y} \left(\bar{J} \frac{\partial}{\partial y} T^4 \right) + \frac{1}{r} \frac{\partial}{\partial r} \left(r\bar{J} \frac{\partial}{\partial r} T^4 \right) \\
&\quad - \theta p \left[\frac{\partial}{\partial y} u_y + \frac{1}{r} \frac{\partial}{\partial r} (r u_r) \right] \\
&\quad - (1-\theta)\ p \left[\frac{\partial}{\partial y} v_y + \frac{1}{r} \frac{\partial}{\partial r} (r v_r) \right]
\end{aligned} \tag{A.8}$$

where $e \equiv (1/\rho) \sum_\alpha \rho_\alpha e_\alpha$ is the energy of the gas mixture and, $\bar{K}$ and $\bar{J}$ are the effective mixture thermal conductivity and radiation diffusion coefficients.

We need an additional equation to form a complete set of equations for N+7 unknowns, θ, ρ_s, F_α ($\alpha = 1,2\ldots,N-1$), ρ, u_y, u_r, v_y, v_r, and T.* This is provided by the specification of the manner in which the solid particles, and hence the solid phase, exchange mass with the gas phase. For our

*It is convenient to solve N-1 equations for the species mass fraction F_α in the gas phase together with another equation for the mass conservation in the gas phase. This latter equation is, of course, obtained from the sum of the N species equations (A.2).

present formulation, we assume that the external volume of the particle is a constant. For combustion reactions this essentially means that the individual particles behave in the manner of the classical unreacted shrinking core model. For the gasification reactions the individual particle mass loss occurs throughout the volume of the particle (c.f., Blake, et al. [1977]).

A.2 NUMERICAL MODEL

The numerical solution of the differential equations is based upon an Eulerian-Lagrangian formulation wherein implicit finite difference techniques are employed (c.f., Blake, et al. [1976, 1977] and Pritchett, et al. [1978]). The Lagrangian character of the code permits the calculation and storage of the histories of particle mass and composition. In the axisymmetric cylindrical coordinate system, the representative solid "particle" used in the Lagrangian formulation of solid particle movement has a toroidal geometry; the cross-section of a torous of the same volume is inversely proportional to the radial distance from the axis. This toroidal "particle" is, of course, representative of a large number of actual particles which, when they are convected to larger radii, will occupy a smaller fraction of the cylindrical volume. In order to model this with the representative "particles" the cross-sectional area of the representative "particle" or toroidal volume must change accordingly. Therefore, a "particle" will have a decreasing cross-section moving away from the axis and an increasing one moving toward the axis. Since we are using constant grid sizes in the radial direction as well as in the vertical direction, the same 2D zone size represents a volume which is also proportional to the mean radial distance. However, a difficulty can occur as a consequence of these kinematic

changes in "particle" cross-section area: too many such "particles" may be required to fill zones far from the axis and too few in zones near the axis. Consequently, when the "particle" cross-sectional area changes beyond some imposed bound, we use numerical procedures to combine or divide these kinematic "particles". This combination or division is not physical but merely defines the representation of the particle such that the same number of representative "particles" occupy each zone of the same solidity.

The numerical treatment of the other equations is the same as in the planar case (c.f., Blake, et al. [1977]).

A.3 SAMPLE CALCULATIONS AND COMPARISON WITH THEORY AND DATA

An illustration of a calculation for the case of an orifice in a fluidized bed distributor plate is shown schematically in Figure A.1. For our present discussion, we assume that the orifice is far from the wall of the bed and that there are a large number of orifices around the orifice in question, the local flow can be approximated by an axisymmetric representation which is bounded by a cylindrical stream surface centered on the orifice. The numerical fluidized bed model predicts the bubble formation and development shown in Figure A.2 for the case of a relatively shallow bed. A comparison of the calculation and experimental data on bubble size and rise velocity shows good agreement between the numerical and experimental results.

Such a comparison between the numerical calculation of the bubble and data can be made using measurements of bubble volume and bubble velocity. These comparisons are shown in Figure A.3 and they illustrate good quantitative agreement between the numerical calculation and theoretical/experimental results. Davidson, et al. [1977] using a model by Harrison and Leung have shown that a simple theory of

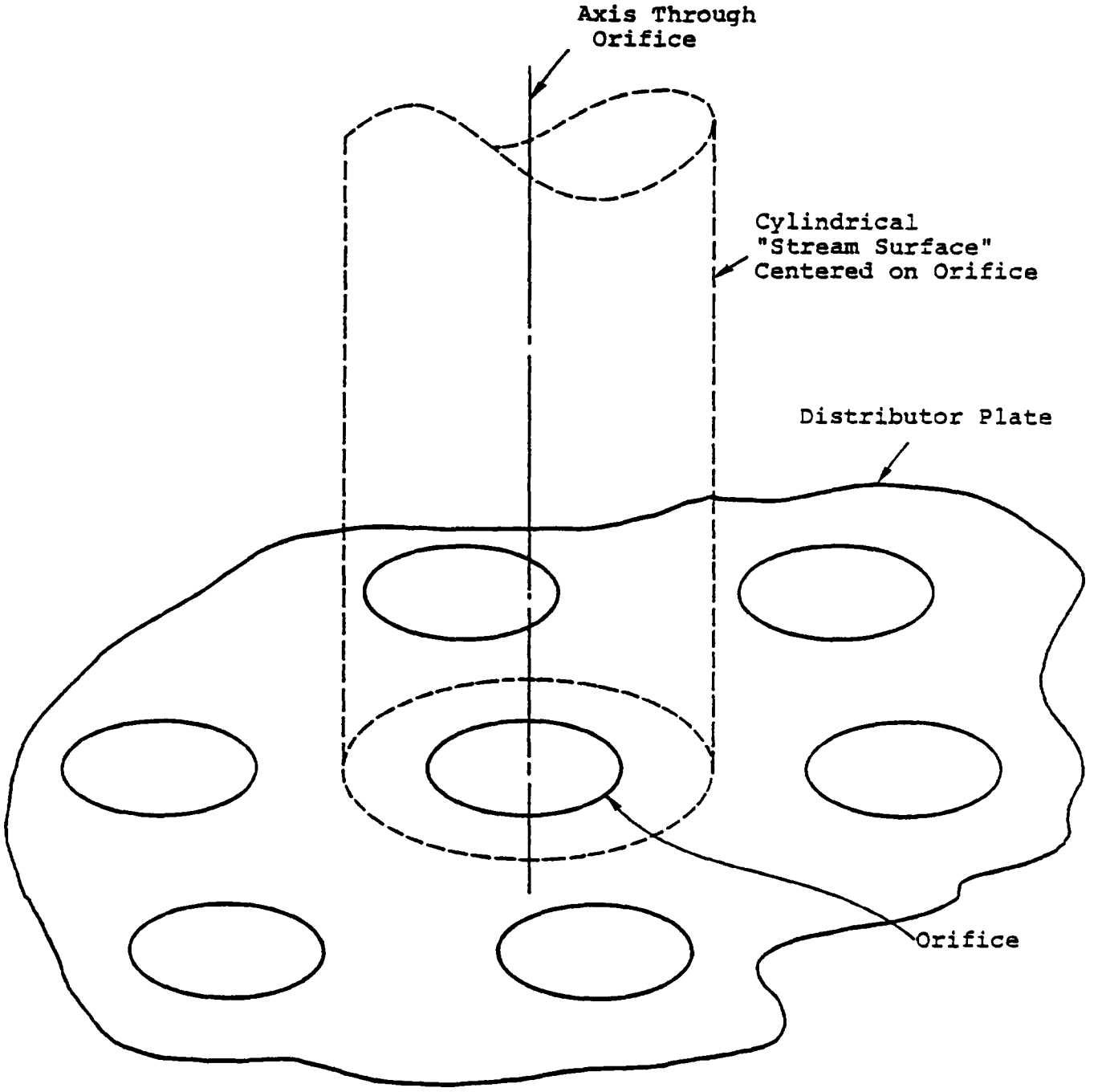

Figure A.1. Axisymmetric region bounded by cylinder centered on orifice of distributor plate.

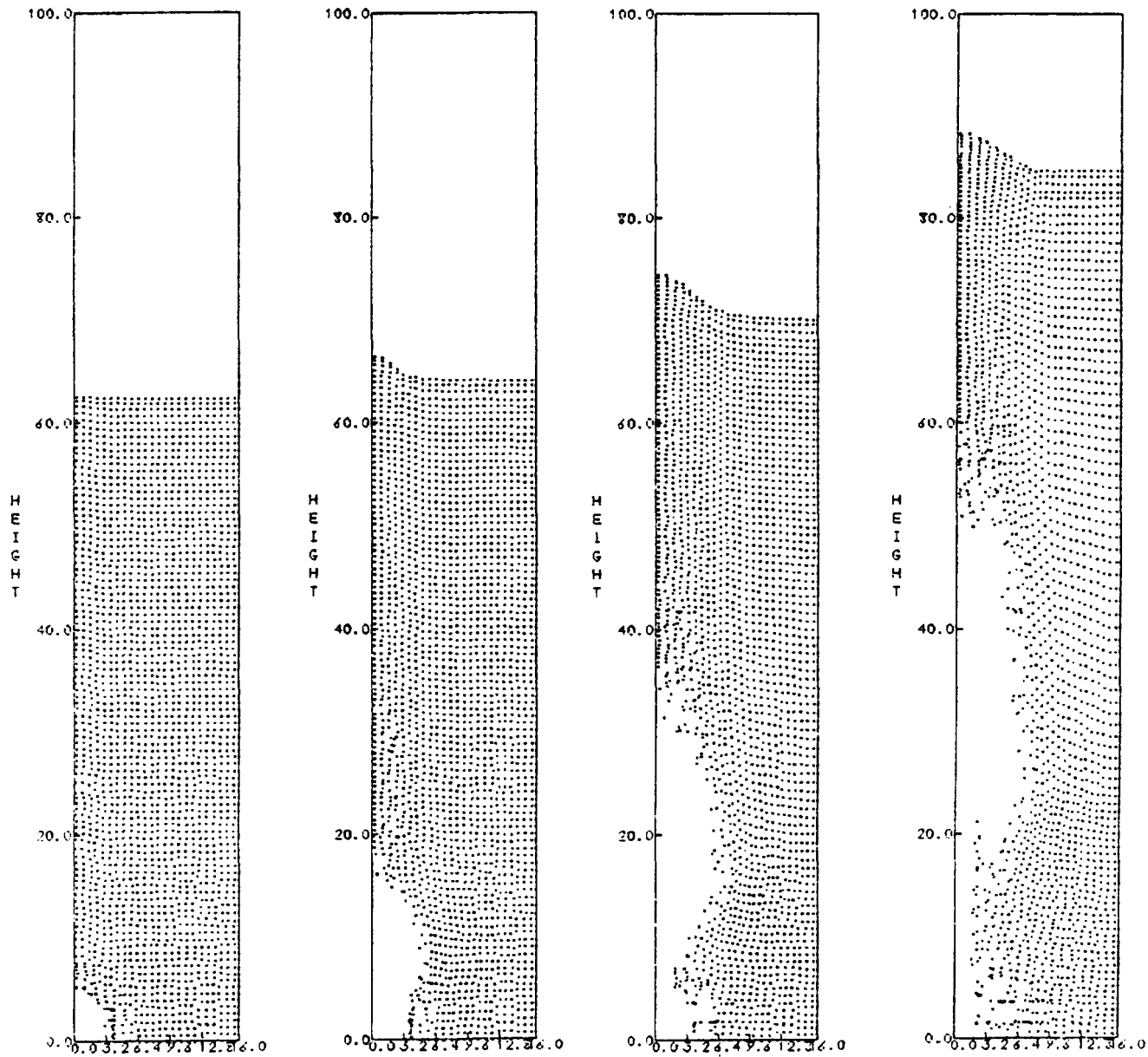

Figure A.2. Jet formation and bubble development within cylinder centered on circular orifice in distributor plate.

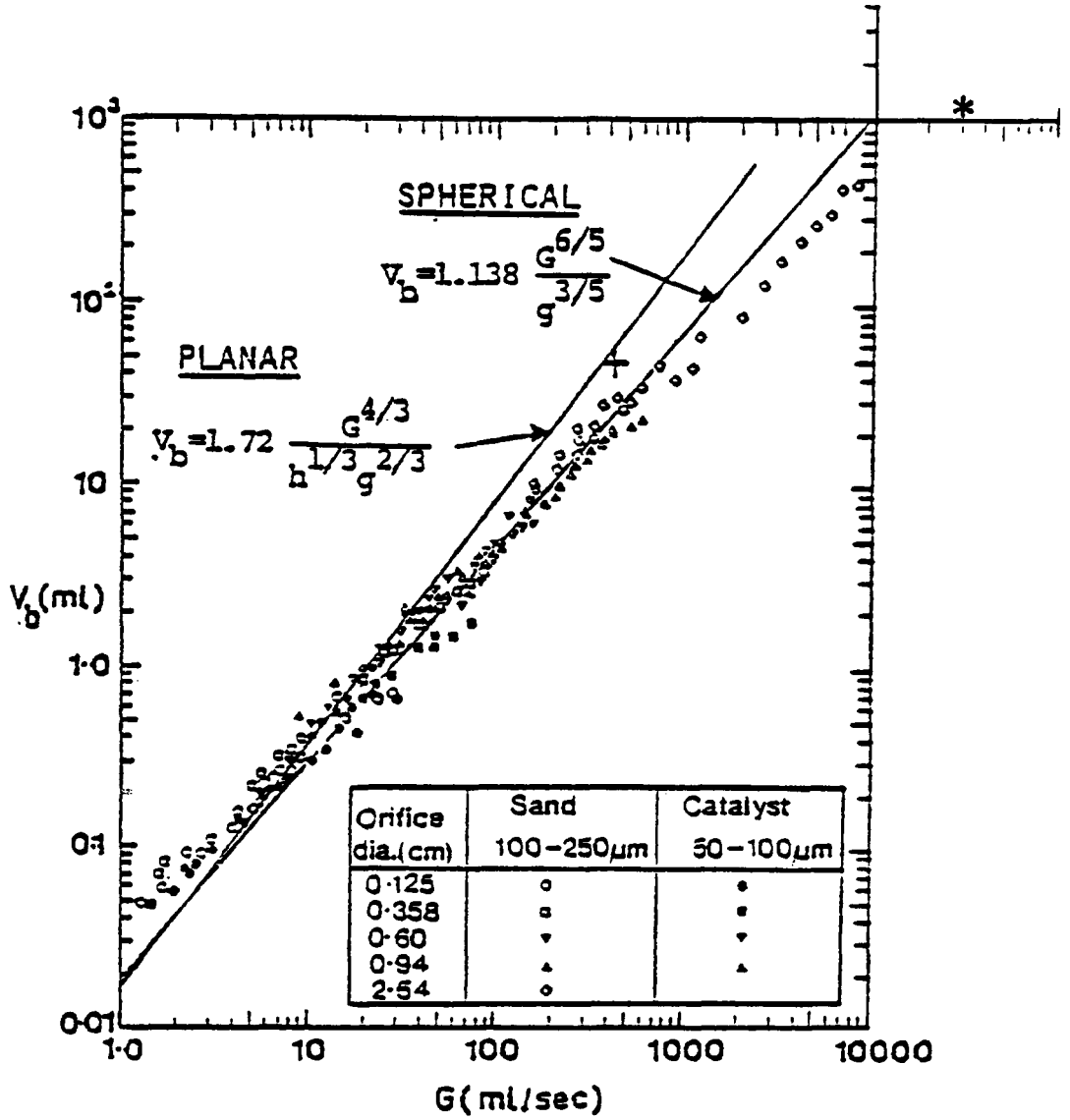

a. Bubble formation at an orifice in an incipiently fluidized bed [Davidson, et al., 1977].

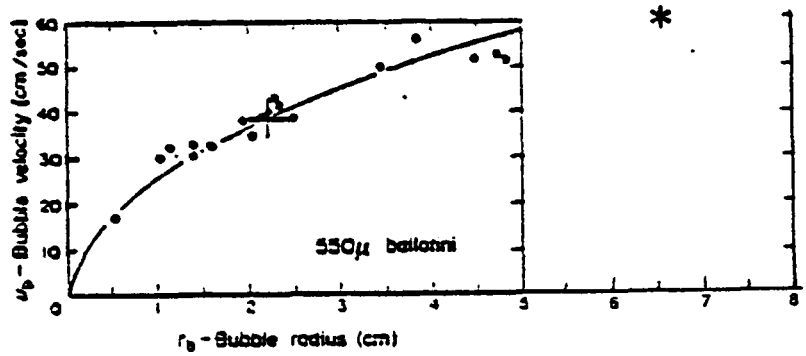

b. Bubble velocity as a function of radius [Rowe, 1971].

Figure A.3. Comparison of numerical calculations with theory/ experiment, 460 μ ballotini: + planar geometry, * spherical geometry.

spherical bubble growth can be used to represent data for bubble development in an incipiently fluidized bed. S^3 has extended that theory to the case of planar bubbles. Such theories relate bubble volume to the volume flow rate through a single orifice. Both axisymmetric and planar theories together with experimental data are shown in Figure A.3a. The axisymmetric bubble volume, determined from the numerical calculation in Figure A.3 is shown as an asterisk in that figure; there is excellent agreement between the data and the numerical result. It is of interest to note that both the numerical calculation and the data indicate a bubble volume which is less than that predicted by the theory. This is not surprising since the theory neglects the important influence of gas diffusion from the bubble into the space between the densely packed particles. In Figure A.3b we provide a comparison between the numerical and experimental results for the case of bubble velocity as a function of equivalent spherical bubble radius in ballotini. Again, the calculated result, indicated by an asterisk, is in good agreement with the data. The relative behavior of planar and cylindrical bubble calculations is also shown in Figure A.3 where the cross indicates the numerical result for planar geometry. That calculation is in agreement with the experimental data in Figure A.3b and with the theoretical curve for planar bubbles in Figure A.3a.

APPENDIX B

SINGLE PARTICLE KINETICS FOR COAL PYROLYSIS

Coal can be thought of as a very large organic-heterocyclic (hydrogen poor) macro-molecule or matrix [Given, 1960], which when heated rapidly will decompose into smaller molecular structures (e.g., H_2O, H_2, CH_4, CO, CO_2, etc.) and residual char (linked carbon structures containing some hydrogen). This process is called pyrolysis or devolatilization and is responsible for a large fraction of the end product fuel gas produced during coal gasification processes. The specific fuel heating value (gas composition) can be strongly influenced by the extent and specific rate processes that occur during pyrolysis and of course, by any subsequent char combustion and gasification reactions.

This Appendix will describe mathematical models for lignite and bituminous coal pyrolysis in inert and hydrogen rich gasification environments. These rate expressions, developed by Howard and his coworkers, include specific effects of the actual pyrolysis and external mass transport rate processes. These expressions represent individual particle and species generation rates as functions of free stream gasifier process variables such as temperature, pressure, species concentration, and particle parameters.

The discussion will include background on the physical and chemical behavior of coals during pyrolysis, a short review of pyrolysis kinetics, and a presentation of the current model.

B.1 PHYSICAL-CHEMICAL ASPECTS OF PYROLYSIS

The process of devolatilization is exceedingly complex, and the mathematical description to follow will by necessity be a much simplified one. As coal undergoes rapid heating, pyrolysis begins with the initial thermal breakdown of the coal matrix into species of significantly lower molecular weight. This decomposition has been reported by many (e.g., Anthony and Howard [1976] and associated references) to initiate at around 350° to 400°C, with very little volatiles evolution occuring at lower temperatures. After initiation, the extent and composition histories of pyrolytic products are strong functions of sample temperature. Anthony and Howard [1976] report that typically 50 percent or more of the initial coal carbon can be volatilized if the process is carried out under sufficient hydrogen pressure. The absolute time scales are such that in the temperature range 1000°-1500°C pyrolysis is completed, typically, in less than 2 sec. What actually happens to the coal particle size and shape and to the compositional histories during this very rapid kinetic development will depend on the coal type (e.g., lignite or bituminous), temperature history, hydrogen pressure, steam-oxygen concentration, total pressure, and particle residence time in the reactor. Such conditions can combine to cause lignites to fracture and cause plastic coals like bituminous to "popcorn" and swell. This behavior will have an obvious effect on the final state of the char produced from pyrolysis, and further it will affect the behavior of the subsequent combustion or gasification reactions.

The pyrolysis of coal and the behavior of the product gases are governed by the competing and inter-connecting phenomena of energy, momentum, and mass transport within and exterior to the coal particle together with the process of thermal decomposition (primary devolatilization) and secondary cracking

chemical reactions. If significant amounts of hydrogen are in the particle exterior environment then hydrocarbon hydrogenation reactions within the particle will also occur. The manner in which these processes affect the total pyrolysis behavior has been briefly discussed by Lewellen [1975]. A synopsis of such discussions provides useful background information for the present model development: Upon examination of the fine structure of coal during pryolysis one finds that the final char porosity increases directly with char formation temperature (at the endpoint of the pyrolysis process). However, for temperatures above 500° to 600°C, the accessability of this void volume (and associated surface area) to transport phenomena rapidly reduces. In the case of plastic coals such as bituminous this temperature range roughly coincides with the beginning of plasticity during which the accessible area reaches a minimum value. The important feature of this observation regarding structural changes is that the structure is intimately connected with the nature of the physico-chemical or transport processes which combine to establish the overall (observable) particle pyrolysis (mass loss) rate. In lignite coals, the above mentioned period of reduction in accessible surface area is accompanied most probably by high internal particle pressures associated with mass transport via diffusional means. Such high pressures would be consistent with the picture of lignite as a non-fluid rigid matrix structure. Whenever the generation rate of volatiles dramatically increases, the rigid lignite structure imposes great resistance to both diffusional and convective material flow. The result of this can be very high internal pressures leading to failure of the lignite structure. This behavior is well known in lignites [Anthony and Howard, 1976].

Conversely the behavior of plastic coals such as bituminous is quite different during devolatilization. Evidence [Ergun, et al. 1959] is such that during the plastic or fluid period, the entire coal particle becomes a liquid-like mass.

Again, as volatiles generation rates increase with rapid heating, both diffusional and convective flows increase dramatically. As this occurs, the resultant pressure forces manifest themselves through bubble formation. The dynamical behavior of plastic coal particles during most of their pyrolysis and the effects of this on observable pyrolysis rate will be strongly influenced by the bubble behavior. Lewellen [1975] has presented a detailed discussion of this process and the effects associated with it.

B.1.1 Mass and Energy Transport Processes

Coal devolatilization can be presumed to be chemically (pyrolysis decomposition reactions) controlled if one finds (experimentally) that the overall (observable) mass loss or pyrolysis rate is independent of particle size [c.f., Anthony and Howard, 1976]. Badzioch and Hawksley [1970] and Howard and Essenhigh [1967] have found this to be the case for particle sizes in the range from 20-74 μm for various operating conditions. It therefore appears that for coal particles smaller than 100 μm transport processes are not important. Certainly this deduction is quite approximate, but it is clear that there is a specific particle diameter or narrow range of diameters above which the influences of energy and/or mass transport will become important. Specific cases of this have been outlined by Anthony and Howard [1976].

(i) External heat transfer is of importance when the coal particles are small and the heating rate is high. Under these conditions there is little temperature gradient in the particle with all of the heat transfer resistance being external to the particle. Pyrolysis rate in this case would increase with decreasing particle size until a size is reached where the equivalent heating rate is so high as to allow

negligible change in pyrolysis rate during heat up. For particles smaller than this, pyrolysis rate will be chemically controlled. Badzioch [1967] has found this size to be approximately 100 μm.

(ii) Internal heat transfer will become significant when the heating rate is low and/or the particles become large enough to allow internal particle temperature gradients. When the gradient is large enough, a pyrolysis reaction wave front will develop in the particle. The rate of movement of this front (consequently the pyrolysis rate) will be controlled by particle heating rate. For heating rates ~ 600° c/s Anthony and Howard [1976] have data indicating that the critical particle diameter for internal heat limitation is in the range 100 to 1000 μm.

(iii) Mass transfer resistances will become important when gradients within and/or exterior to the particle become significant. Essenhigh [1963] was able to experimentally correlate devolatilization times tv with initial particle diameter, i.e.,

$$t_v = K_v d^2 \quad , \qquad (B.1)$$

where K_v is a direct function of the coal volatile content and an inverse function of char permeability. This correlation was found to hold quite well with particles in the size range of 295 to 4760 μm, but breaks down when extrapolated below about 150 μm. Such a rate model is consistent with the picture of a coal particle devolatilizing according to a shrinking core mode.

Below 150 μm then, mass transfer effects, although not necessarily negligible, are expected to be in competition with and be governed by other descriptions besides the shrinking core picture.

In the discussions to follow, the emphasis will be on the pyrolysis of particles in the size range of less than 100 μm and under conditions of very high heating rates (e.g., $10^4 \sim 10^5$°C/sec). From the above discussion this essentially precludes internal particle heat transfer effects and, consequently, our attention will be focused on the simultaneous affects of mass transport and chemical reaction (primarily pyrolysis decomposition and associated secondary reactions) upon the observable pyrolysis rate.

B.2 REACTION KINETICS FOR RAPID DEVOLATILIZATION

As previously mentioned the pryolytic decomposition of coal is very complex, and, to date, no detailed or confirmed mechanisms have been established for this process. It is generally understood however that coal is composed of a complex matrix of aromatic and aliphatic hydrocarbon rings interconnected by aliphatic and olefinic chains. This matrix is also liberally substituted with oxygen, nitrogen, and sulfur atoms and their functional groups. Molecular structures of this type are known to thermally decompose at specific characteristic temperatures and rates which are a function of the bond energies and structural orientations involved. In terms of a chemical kinetics description this means that each structural decomposition reaction possesses a unique activation energy and velocity coefficient (pre-exponential factor), in the corresponding rate expression. With this being the case, any approximately descriptive kinetic model of pyrolysis must reflect the existence of an almost infinite and simultaneous parallel set of decomposition reactions with the possibility of some competing (interconnecting) reactions as well. Several investigators have taken data and proposed reaction rate models, and some of these are discussed below.

B.2.1 Rate Models

The approach that many researchers have taken to this problem is to assume that the entire pyrolysis decomposition process is first order in the unreacted material remaining in the coal. This is usually expressed as,

$$\dot{r}_v = k_v \, (V^* - V) \ , \qquad (B.2)$$

where $\dot{r}_v$ = volumetric rate of generation of total volatiles [cm^3/sec]

k_v = rate constant $[sec]^{-1}$

V = volatiles lost from particle up to time t

V^* = value of V as $t \to \infty$ [cm^3].

From a mechanistic viewpoint this approach is quite unsatisfactory in that it lumps the entire spectrum of reactions into a single value of activation energy and preexponential rate constant. There has been limited success in the use of Eq. (B.2) for a range of different coal pyrolysis data. This can be seen by examining Figure B.1 and Table B.1 taken from the Anthony and Howard [1976] review.

Several orders of magnitude variation in the rate constants over the same temperature range is quite evident. Anthony and Howard [1976] point out that some, but certainly not all, of this variation is due to differences in coal rank and equipment used in the experiments. These variations are quite prevalent in <u>all</u> data on coal pyrolysis. Many apparent phenomena can be traced to affects of experimental conditions. For example, many investigators (Jüntgen and Van Heek [1968], and Kobayashi [1972]) have found significant increases of volatile yield with increased heating rate and have extended generalized rate models including this effect. For example Jüntgen and Van Heek propose,

$$r_{vi} = (k_{o,i}/m)\ (V^*_i - V_i)\ \exp\ (E_i/RT) \qquad (B.3)$$

for each evolved species i and with $m = \frac{dT}{dt}$, being the appropriate heating rate. However, as pointed out by Anthony and Howard [1976], experimental conditions for changing heating rates, e.g., a change in residence time of the coal particles in the heating zone, can effectively change the residence time of the volatiles in contact with the devolatilizing coal particles. This can have an effect on the extent to which the

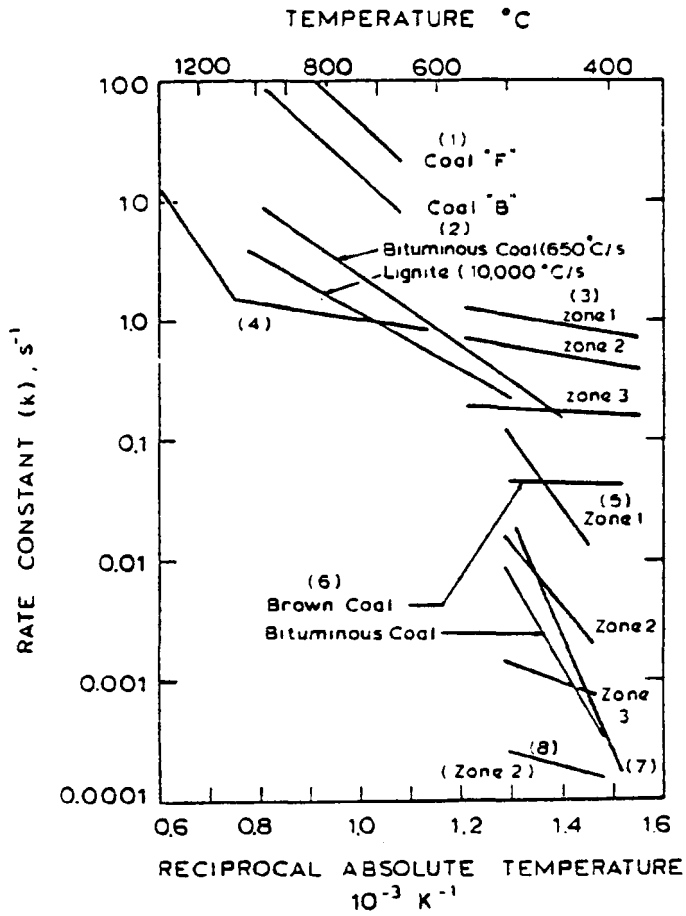

Figure B.1. Comparison of simple first-order coal devolatilization rate constants from different investigators [(1) Badzioch and Hawksley [1970], (2) Anthony, et al. [1975], (3) Shapatina, et al. [1960], (4) Howard and Essenhigh [1967], (5) Stone, et al. [1954], (6) Van Krevelen, et al. [1951], (7) Boyer [1952] and (8) Wiser, et al. [1967]].

TABLE B.I. COAL PROPERTIES AND DEVOLATILIZATION RATE PARAMETERS IN FIGURE B.1

Investigators	Coal	*VM* (MF)*	*VM* (MAF)†	*E*, kcal/mole	k_0, s^{-1}	Comments
Badzioch and Hawksley (1970)	B NCB 902	35.2	36.4	17.8	1.14×10^5	
	F NCB 601	34.9	35.3	17.8	3.12×10^5	
Boyer (1952)	St. Fontaine bituminous	—	36.0	45	1.00×10^{11}	Reported by Yellow (1963)
Howard and Essenhigh (1967)	Pittsburgh Seam bituminous	35.9	37.4	27.7	4.92×10^4	$T > 1\,060$°C
				3.4	5.37	$T < 1\,060$°C
Shapatina et al. (1960)	Moscow district brown coal	34.5	50.2	3.6	11.0	Zone 1 (0 — 0.06 s)
				3.8	6.63	Zone 2 (0.06 — 0.1 s)
				1.0	0.37	Zone 3 (0.1 — 180 s)
Stone et al. (1954)	Pittsburgh Seam bituminous	40.7	42.2	27.3	5.41×10^6	Zone 1
				24.4	1.10×10^5	Zone 2
				7.0	0.131	Zone 3
Van Krevelen et al. (1951)	Brown coal	—	51.0	0.7	0.07	Values corrected by Jüntgen and Van Heek (1970)
	Low-rank bituminous	—	39.5	32.5	1×10^7	
Wiser et al. (1967)	Utah bituminous	47.5	—	15.0	47.5	Zone 2 (> 3 600 s)
Anthony et al. (1975)	Pittsburgh Seam bituminous	40.5	46.2	13.3	1.80×10^3	
	Montana lignite	40.3	46.2	20.0	2.90×10^5	Excluding cooling
				11.1	2.83×10^2	Including cooling

* Moisture free.
† Moisture and ash free.

volatiles undergo secondary reactions such as cracking, etc. A difference in yield will occur under such varying circumstances. Further, variations in initial particle size can lead to transport limitations and therefore disguise the effective pyrolysis rate. The nature of the experimental gas particle regime, e.g. entrained flows, fixed beds, or fluidized beds all can have residence time and temperature variation effects which in turn affect total yield. To arrive at a useful mathematical model for pyrolysis in real gasifiers, several investigators have proposed complex competing type reaction kinetic mechanisms to account for residence time, temperature history and secondary, cracking reaction effects. The following Figure B.2 from Anthony and Howard [1976] is a brief schematic description of the various approaches taken for these "revised" models.

The approach adopted in this study is one proposed by Pitt [1962] originally and later generalized by Anthony, et al. [1975]. In this model pyrolysis is treated as the thermal decomposition of coal by means of an infinite number of independent first order irreversible reactions, each having its own activation energy. For the sake of simplicity, all reactions are assumed to have the same pre-exponential factor, k_0. Anthony, et al. [1975] proposed this model in the form as follows for the rate of production of species i;

$$\dot{r}_i = k_i \, (V^*_i - V_i) \ , \qquad (B.4)$$

where V_i = the weight percent of as received coal of volatiles formed from the i^{th} reaction of an infinite number of reactions. In the limit where $i \to \infty$

$$\mathring{r}_T = \int d\mathring{r}_T = \int_0^\infty \mathring{r}(E) f(E) \, dE \qquad (B.5)$$

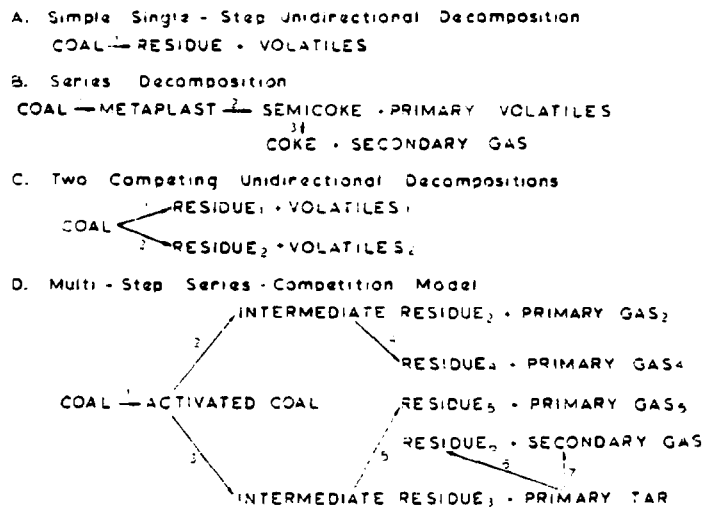

Figure B.2. Coal pyrolysis models [A. Equation (B.2); B. Van Krevelen [1961]; C. Kobayashi [1972]; D. Reidelbach and Summerfield [1975]].

where

$$\int_0^\infty f(E)\,dE = 1 \tag{B.6}$$

In this form an infinite number of discreet reactions with discreet activation energies has been replaced with a class of reactions associated with a <u>continuous</u> distribution of activation energies f(E). In this formalism, the now continuous function $\mathring{r}_T$ takes the general form

$$\mathring{r}_T = k_\circ\ (V^* - V) \int_\circ^\infty e^{-E/RT}\ f(E)\,dE \tag{B.7}$$

which is based upon the following manipulations:

$$\mathring{r}_i = d\mathring{r}_T = \mathring{r}_T dF = \mathring{r}_T f(E)\,dE \tag{B.8}$$

$$\int d\mathring{r}_T = \sum_{i=1}^{\infty} k_i\ (V^*_i - V_i) = \mathring{r}_T \tag{B.9}$$

We define a <u>continuous</u> distribution of activation energies,

$$k_i \equiv k(E) = k_\circ e^{-E/RT} \tag{B.10}$$

so that (B.7) follows.

B.2.2 Correlations and Data for Individual Evolved Species

Theoretical reaction rate expressions can be written for each chemical species evolved during pyrolysis following Eq. (B.7); i.e.,

$$r_{T_\alpha} = \left\{ \int_0^\infty k\,(E) f\,(E) dE \right\} (V_\alpha^* - V_\alpha) \qquad (B.11)$$

for each species α. Again, this is equivalent to saying that each evolved species is formed as a result of an infinite number of first order irreversible decomposition reactions. In fact, Suuberg, et al. [1977] have taken this approach in measuring pyrolysis kinetics for individual species from Montana lignite and Pittsburgh seam bituminous coals. That study uses the technique of very rapid heating or pulverized coal samples on an electrical grid to produce pyrolysis in an inert gas environment. The experiments are done on a batch basis and all products and residuals are retained and analyzed. This data on lignite and bituminous coals indicates that the application of Eq. (B.11) must be modified depending on the coal type. For example, in the case of lignite, the production of a specific species appears to be characterized by discreet activation energies rather than a continuous distribution. This behavior is surmised from Figures B.3 and B.4 taken from Suuberg, et al. [1977] for individual yields as a function of peak pyrolysis temperature. Each yield plateau represents a rate process occurring at a specific activation energy. For this reason, in the case of lignite pyrolysis, individual species yield rates will be modeled with a single activation energy or at most a linear combination of a few different activation energies, not a continuous function or distribution as in Eq. (B.11). In S^3 modeling the kinetic parameters and activation energies as obtained by Suuberg, et al. [1978] will be used for lignite pyrolysis in inert environments; see Table B.II.

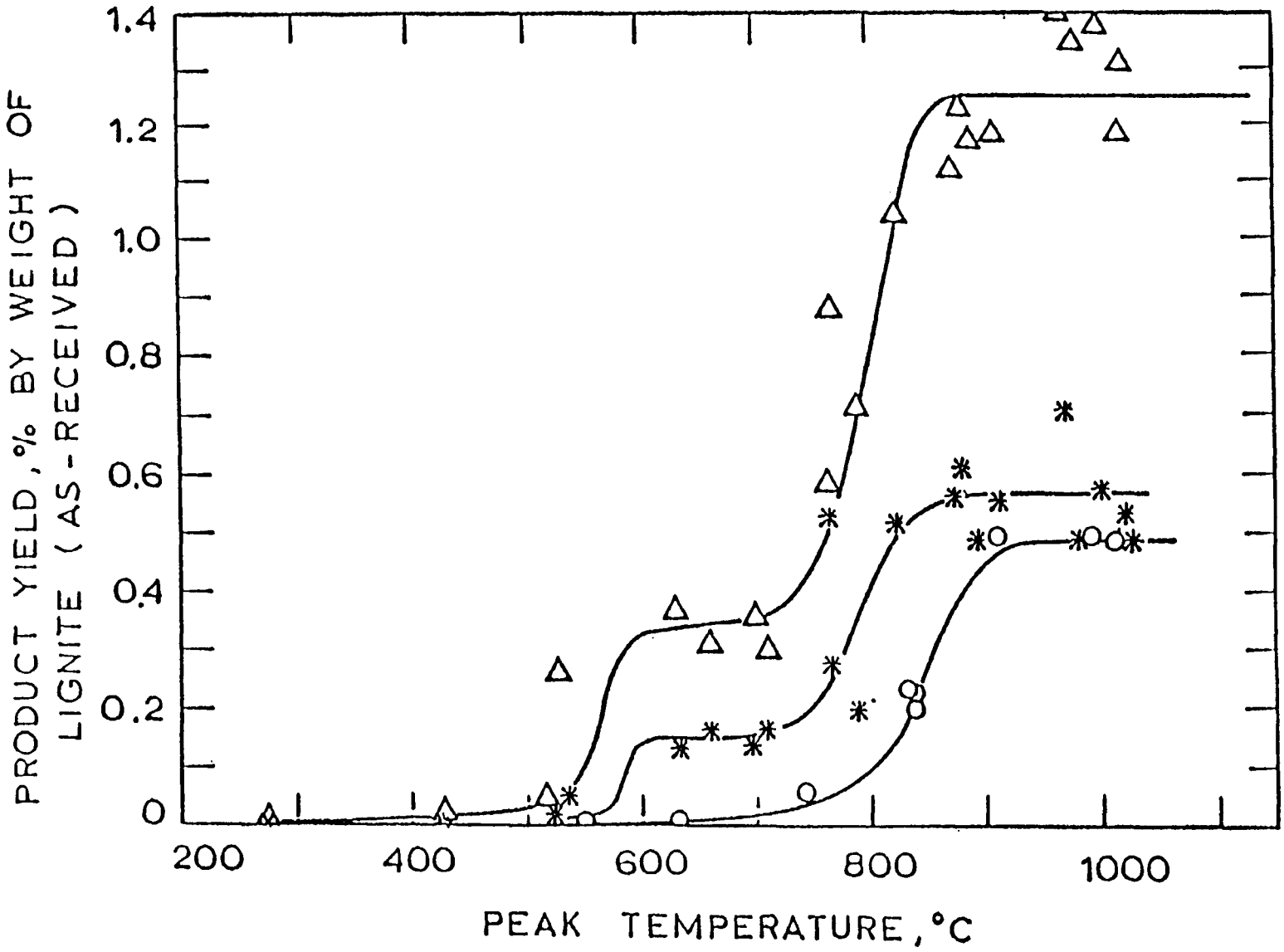

Figure B.3. Yields of methane, ethylene and hydrogen from lignite pyrolysis to different peak temperatures [(Δ) CH_4; (*) C_2H_4; (o) H_2. Pressure = 1 atm (helium). Heating rate = 1000°C/s].

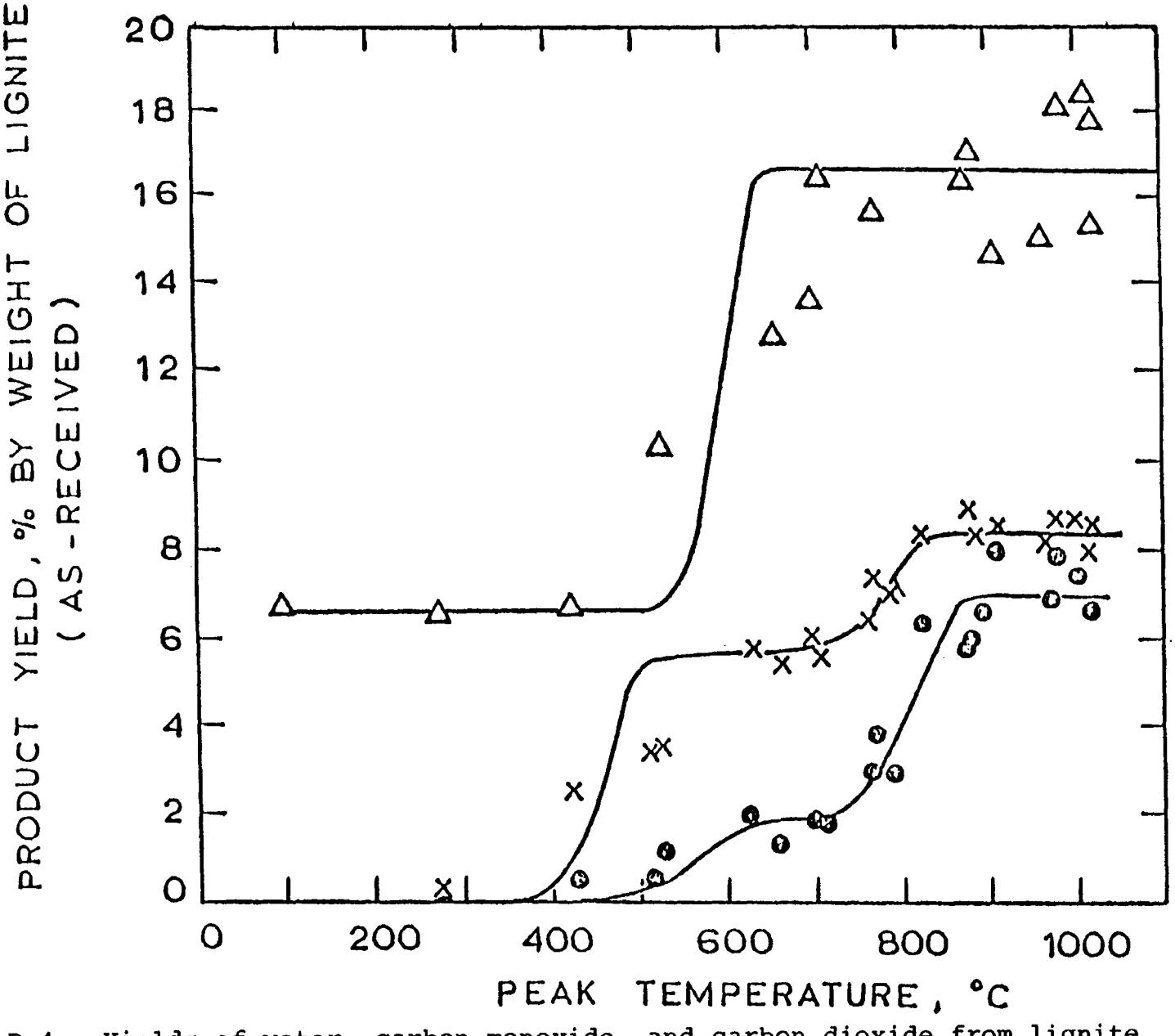

Figure B.4. Yields of water, carbon monoxide, and carbon dioxide from lignite pyrolysis to different peak temperatures [(Δ) H_2O; (x) CO_2; (o) CO. Pressure = 1 atm (helium). Heating rate = 1000°C/s].

Table B.II. Kinetic Parameters for Lignite Pryolysis

Product	Stage	E_i, kcal/mole	log (k_{i0}/s^{-1})	V_i^*, Wt.% of lignite (as-received)
CO_2	1	36.2	11.33	5.70
	2	64.3	13.71	2.70
	3	42.0	6.74	1.09
CO	1	44.4	12.26	1.77
	2	59.5	12.42	5.35
	3	58.4	9.77	2.26
CH_4	1	51.6	14.21	0.34
	2	69.4	14.67	0.92
C_2H_4	1	74.8	20.25	0.15
	2	60.4	12.85	0.41
HC[a]		70.1	16.23	0.95
Tar	1	37.4	11.88	2.45
	2	75.3	17.30	2.93
H_2O		51.4	13.90	16.5
H_2		88.8	18.20	0.50
Total				44.0

a. Hydrocarbons other than CH_4, C_2H_4 and Tar

In contrast to the above lignite behavior, pyrolysis of bituminous coal is in agreement with the concept of a distribution of activation energies. Preliminary data on bituminous, shown in Figure B.5, taken from Bush, et al. [1977], indicate smooth yield versus peak temperature dependence with no steps. Based on this it would appear necessary to model the species pyrolysis rates in this case using a continuous distribution of activation energies for each species as in Eq. (B.11). The data in Figure B.5 was obtained by Suuberg. As of now, no actual kinetic parameters are available from MIT on the bituminous coal; i.e., analogous to Table B.II. However, this should be forthcoming.

The above discussion applies to pyrolysis in inert environments. Many investigators (Dent [1944], Fieldkirchner and Linden [1963], Schroeder [1962], Hiteshue, et al. [1962], Johnson [1971] and others) have observed and taken data of coal pyrolysis in hydrogen rich environments at various pressures of ambient hydrogen. This data shows a behavior which is quite different from inert pyrolysis. Depending on the pressure, higher total volatile yield, dominated by methane, can be produced in hydropyrolysis. The time scale and rate of production of this so-called "rapid rate methane" are on the same order as ordinarv (inert) pyrolysis at the same heating rates. There have been several hypothesis as to the nature of the mechanism involved in such a process. A lengthy discussion of these theories will not be presented here, and the reader is referred to the Anthony and Howard [1976] review for a detailed account. However, the general nature of these hypotheses may be discussed. Two leading mechanisms have been hypothesized to provide some correlation of the experimentally observed temperature and pressure effects on volatile yield in hydropyrolysis; (1) an active species model which postulates that coal pyrolysis

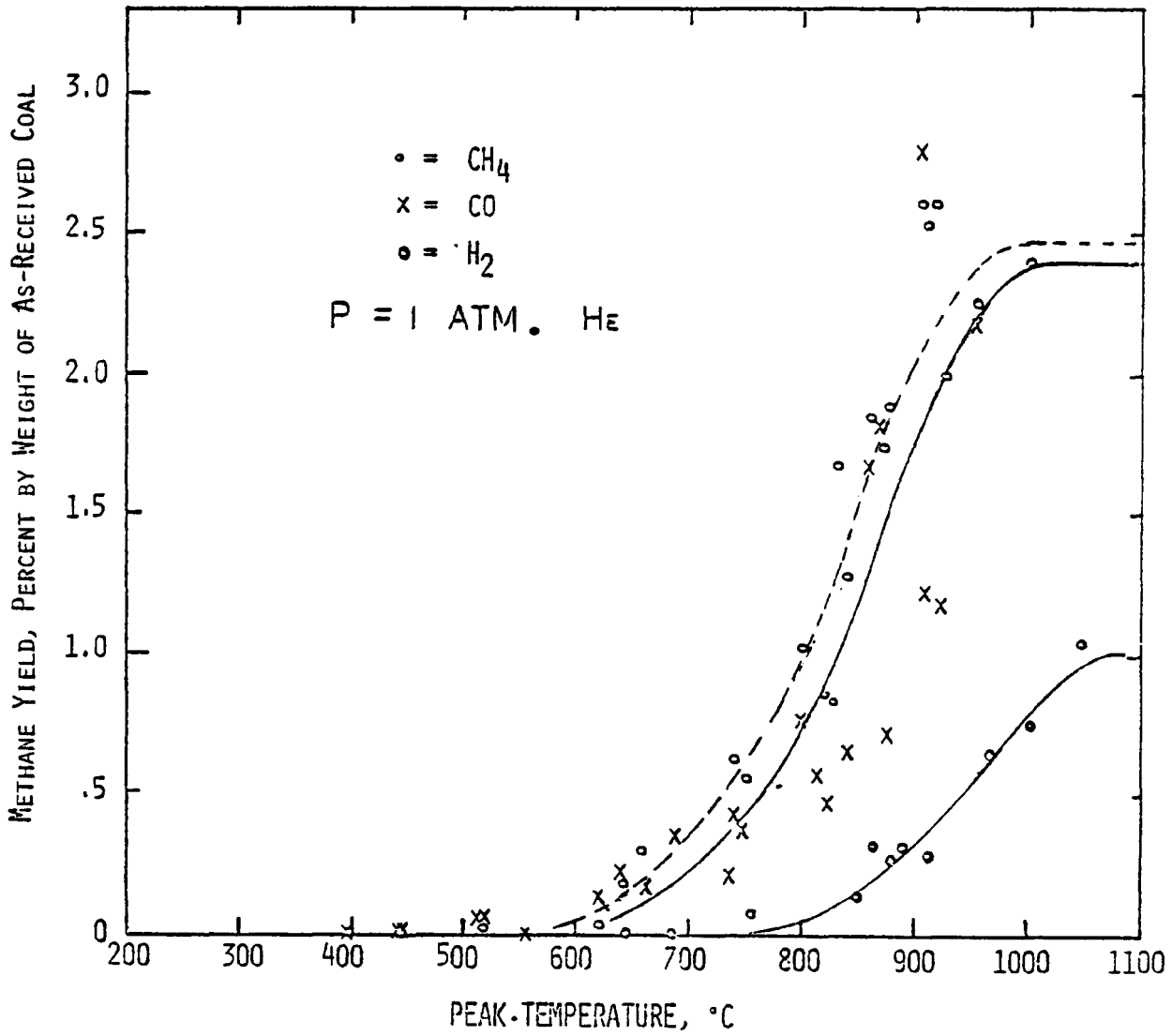

Figure B.5. Yields of principal gaseous products from bituminous coal pyrolysis at various peak temperatures in the batch reactor.

produces, along with volatiles, activated carbon sites which can produce methane upon reaction with hydrogen or a relatively inactive char by cross linking; and (2) a sequential reaction model proposed by Anthony and Howard [1976], which involves the reaction of ambient hydrogen with reactive volatile species immediately after they have been formed by ordinary pyrolytic decomposition. In this manner these volatiles become stable methane and higher molecular weight hydrocarbons (which of course can hydrocrack to produce more methane). In the present model effort, this second hypothesis will be adopted primarily due to its apparent ability to interpret the effect of pressure on the rate of coke production. Both hypotheses include temperature and hydrogen partial pressure effects through the use of a global kinetic expression of the type.

$$r_{CH_4} = k_o e^{-E/RT} f(P_{H2}) \qquad (B.12)$$

where

$$f(P_{H_2}) \sim P_{H_2} \qquad (B.13)$$

However, when one examines the influence of total system pressure on volatile yield (Figure B.6, from Anthony and Howard, [1976]) it can be seen that increased pressure results in a dramatic decrease in total volatile yield (weight loss) for both inert and hydrogen environments up to a total of about 10 atm. This phenomenon is associated with the retardation of the transport of volatile species from within the coal particles to the exterior, allowing increased opportunity for them to participate in coking reactions. With further increases in pressures, the influence of hydrogen becomes apparent. Volatile yield now begins to <u>increase</u> with H_2 pressure. A possible explanation, suggested by Howard, is that the increased presence of hydrogen is interfering with the cross-linking, coking type reactions by directly hydrogenerating the highly reactive and newly formed volatile species.

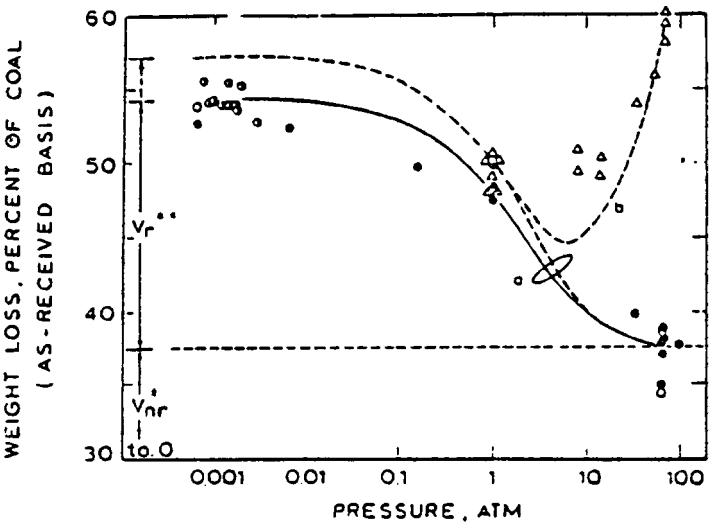

Figure B.6. Effect of pressure on weight loss from Pittsburgh Seam bituminous coal heated in hydrogen and helium atmospheres [Anthony, et al. [1976], Ireland Mine coal, final (holding) temperature, 1000°C, residence time, 5 to 20 s; mean particle diameter, 70 μm; (o) helium, nominal heating = 10,000°C/s; (o) helium, nominal heating rate = 3,000°C/s; (o) helium, nominal heating rate = 650° to 750°C/s; (Δ) hydrogen, nominal heating rate = 750°C/s; V_r^{**} = 17.0 percent of original coal; (dashed) V_r^{**} = 20.0 percent of original coal, corrected for cracking deposition on sample holder; V_{nr}^* = 37.2 percent or original coal].

Of course, the process of "rapid rate methane" formation is still the subject of much study. For our purposes we will assume that during hydropyrolysis the dominant rate of formation of CH_4 (and consumption of H_2) can be represented by the first order form of Eqs. (B.12) and (B.13). Rate constants, activation energies, and stoichiometry will be estimated from the data produced by Suuberg and Howard [1977].

B.3 INTERPHASE MASS EXCHANGE DURING PYROLYSIS

The previous section indicates that some limited experimental data is now available to describe the evolution of single species from Montana Lignite and Pittsburgh bituminous coal. Mathematical expressions are needed for the rate of evolution of species from single particles to ambient environments typical in entrained flow gasifiers. Such expressions will incorporate that data in an appropriate manner.

The previous correlations for pyrolysis of lignite are based on the following form

$$\frac{dV_\alpha}{dt} = k_\alpha \, (V_\alpha^* - V_\alpha), \text{ for species } \alpha \qquad \text{(B.14)}$$

$$k_\alpha = k_{\alpha 0} \, e^{-E_\alpha / RT_p}, \qquad \text{(B.15)}$$

where

V_α = yield of species α at time t expressed as fractional weight loss of the as received coal,

V_α^* = fractional weight loss of species α at $t \to \infty$ expressed as net fraction of as received coal.

The data in Suuberg [1977], Suuberg, et al. [1977], Suuberg, et al. [1978] (c.f., Figures B.4 and B.5) show that for lignite, an equation like (B.14) represents one or more stages in the pyrolysis of each species. Hence devolatilization of a species is described by a linear combination of rates for each species with a distinct activation energy for each element in the sum. In the S^3 model, each of these distinct elements will be treated as a separate species during pyrolysis. When the pyrolysis step is complete, each "sub-species" will be summed to give the entire "total" species yield.

To appropriately use the correlational forms of Eqs. (B.14) and (B.15) some structure must be given to what is

being called a coal particle. In this initial phase of modeling, the coal will be taken as spherical and of unchanging size. Also, the following assumptions regarding the rate processes during rapid entrained flow pyrolysis will be made.

1. Particle sizes will be in the 20-75 μm range, resulting in uniform particle interior temperatures. This will be a good assumption for the high heating rates (10^4-10^5°C/sec) of entrained flow gasifiers.
2. The pyrolysis process will be taken as quasi-static with respect to boundary conditions on species mass conservation equations.
3. Other rate processes such as heterogeneous combustion and gasification will be considered slow enough to not impinge on basic pyrolysis.
4. The internal coal particle physical mass transfer processes are assumed to be dominated by flux of pyrolytic products to the particular surface. Consequently, the mechanisms of pyrolysis, hydrogenation, polymerization (coke formation) and particle-gas transport of reactive volatiles are parallel phenomena which comprise the quantitative reaction rate K_α (c.f., Suuberg [1977] or Anthony and Howard [1976]).

The following definitions will be used

$V_p = \frac{4}{3} \pi r_0^3 \equiv$ the fixed coal particle volume,

$\rho_c \equiv$ the known coal particle density (as received basis,

$\rho_{s\alpha} = (V_\alpha^* - V_\alpha)\ \rho_c \equiv$ mass concentration of species α (as identified in the gas phase) in the coal particle which has yet to be evolved.

The last definition further assumes that a single coal particle is uniformly representative of the sample batch from which V_α^* is determined. We can now write for a single particle the basic rate of evolution (locally) for species α due to pyrolysis, i.e.,

$$r_\alpha = k_\alpha \rho_{s\alpha} \ . \tag{B.16}$$

Again k_α is, in general, influenced by several competing phenomena. For the reactive volatiles we expect that

$$k_\alpha \sim \frac{\dot{Q}_\alpha}{K_{M_\alpha} + K_{1_\alpha} + K_{2_\alpha} P_{H_2}}$$

where we use Suuberg's notation and where $\dot{Q}_\alpha$ is the rate of formation of a reactive volatile, K_{M_α} is the mass transfer coefficient, K_{1_α} is the rate of secondary repolymerization and $K_{2_\alpha} P_{H_2}$ is the rate of hydrogenation. For the present, there is not a sufficient data base and correlation of that data to provide a complete definition of these individual coefficients. Consequently we will primarily deal with the overall values of k_α defined for specific ambient environments and discussed in Section B.2. When additional correlations are available from Howard and his coworkers to quantify ($\dot{Q}_\alpha$, K_{M_α}, K_{1_α}, K_{2_α}) for more general environments we will incorporate that additional structure into our representation of pyrolysis.

The rate of evolution of species α from a single particle (B.16) must be summed over individual particles to provide the appropriate source terms in our continuum representations of the solid and gas phases. The above rate is based upon a unit volume of the coal particle; it provides the following interphase exchange rate based upon the coal particle surface area

$$R_{\alpha_D} = \frac{1}{3} k_\alpha \rho_{s\alpha} \tag{B.17}$$

Further, if all particles are, <u>locally</u>, the same, then the use of the weighting function $G(|x_i - y_i|)$ (c.f., Blake, <u>et al.</u> [1976, 1977]) gives the interphase exchange rate, associated with pyrolysis as,

$$S_{\alpha_D} = \sum_P G(|x_i - y_i|) \, 4\pi r_0^2 \, R_{\alpha_D} \tag{B.18a}$$

or

$$S_{\alpha_D} = (1-\phi) \frac{3}{r_0} R_{\alpha_D} = (1-\phi) \frac{k_\alpha \rho_{s\alpha}}{r_0} \tag{B.18b}$$

For the more general case of locally different particles, the former of these two equations must be used, with r_0 and R_{α_D} having distinct values for each particle within the radius of the weighting function.

REFERENCES

Anthony, D. B. and J. B. Howard [1976], AIChE J., 22(4), p. 625.

Anthony, D. B., J. B. Howard, H. C. Hottell, and H. P. Meissner [1975], "Rapid Devolatilization of Pulverized Coal," Fifteenth Symposium (International) on Combustion, p. 1303, The Combustion Institute, Pittsburgh, Pennsylvania.

Badzioch, S. and P. O. Hawksley [1970], "Kinetics of Thermal Decomposition of Pulverized Coal Particles," Ind. Eng. Chemical Process Design Development, 9, p. 521.

Blake, T. R., S. K. Garg, H. B. Levine and J. W. Pritchett [1976], "Computer Modeling of Coal Gasification Reactors," Annual Report, June 1975 - June 1976, U. S. Energy Research and Development Administration Report FE-1770-15.

Blake, T. R. [1977], "Computer Modeling of Coal Gasification Reactors," Quarterly Progress Report, July 1977 - September 1977, U. S. Energy Research and Development Administration Report FE-1770-35.

Blake, T. R., D. H. Brownell, Jr., S. K. Garg, W. D. Henline, J. W. Pritchett and G. P. Schneyer [1977], "Computer Modeling of Coal Gasification Reactors," Annual Report. June 1976 - June 1977, U. S. Energy Research and Development Administration Report FE-1770-32.

Blake, T. R., D. H. Brownell, Jr., and G. P. Schneyer [1978], "A Numerical Simulation Model for Entrained Flow Coal Gasification, I. The Hydrodynamical Model," Proceedings Miami Intl. Conf. on Alternative Energy Sources, December 1977, Miami, in press.

Boyer, M. S. F. [1952] , Comput. Rend. Assoc. Tech. de l'Indus. du gaz en France Congres., p. 653.

Bush, T. W., J. B. Howard, S. Kenda, D. Mead, W. A. Peters, and E. M. Suuberg [1977], MIT, Dept. of ChE., Semi-Annual Progress Report for January 1, 1977 - June 30, 1977 to ERDA under Contract No. EX-76-A-01-2295.

Davidson, J. F., D. Harrison and J. R. F. Guedes de Carvalho [1977], Annual Review of Fluid Mechanics, 9, Annual Reviews, Palo Alto, California.

Dent, F. J. [1944]. "The Production of Gaseous Hydrocarbons by the Hydrogenation of Coal," Gas J., 244, p. 502.

Essenhigh, R. H. [1963], "The Influence of Coal Rank on the Burning Times of Single Captive Particles," J. Eng. Power, 85, p. 183.

Ergun, S., H. J. O'Donnell, and B. C. Parks [1959], "Microscopic Studies of Rate of Thermal Decomposition of Petrographic Components of Coal," Fuel, 38, p. 205.

Feldkirchner, H. L. and H. R. Linden [1963], "Reactivity of Coals in High-Pressure Gasification," Ind. Eng. Chem. Process Design Develop., 2, p. 153.

Given, P. H. [1960], "The Distribution of Hydrogen in Coals and its Relation to Coal Structure," Fuel, 39, p. 147.

Howard, J. B., and R. H. Essenhigh [1967], "Pyrolysis of Coal Particles in Pulverized Fuel Flames," Ind. Eng. Chem. Process Design Develop., 6, p. 74.

Hiteshue, R. W., S. Friedman, and R. Madden [1962], "Hydrogenation of Coal to Gaseous Hydrocarbons," RI 6027, Bureau of Mines, Dept. of Interior, Washington, D. C.

Johnson, J. L. [1971], "Means of Relating Coal Characteristics to Chemical Engineering Data," Seminar on Characterization and Characteristics of U.S. Coals for Practical Use, Pennsylvania State University, University Park, October 25-28, 1971.

Juntgen, H. and K. H. Van Heek [1968], "Gas Release from Coal as a Function of the Rate of Heating," Fuel, 47, p. 103.

Kobayashi, H. [1972], "Rapid Decomposition Mechanism of Pulverized Coal Particle," M.S. Thesis, Dept. of Aeronautics and Astronautics, MIT, Cambridge, Massachusetts.

Lenzer, R. C., P. E. George, J. F. Thomas and N. M. Laurendeau [1976], "Gasification in Pulverized Coal Flames," Annual Progress Rbport July 1975 - June 1976, U. S. Energy Research and Development Administration Report FE-2029-4.

Lewellen, P. C. [1975], "Product Decomposition Effects in Coal Pyrolysis," M.S. thesis, Dept. of Chemical Engineering, MIT, Cambridge, Massachusetts.

Pritchett, J. W.,T. R. Blake and S. K. Garg [1978], "A Numerical Model of Gas Fluidized Beds," in press, AIChE Progress Symposium Series, Fluidization, Applications to Energy Conversion.

Pitt, G. J. [1962], "The Kinetics of the Evolution of Volatile Products from Coal," Fuel, 41, p. 267.

Quan, V. [1972], Intl. J. Heat and Mass Trans., 15, p. 2173-86.

Reidebach, H. and M. Summerfield [1975], "Kinetic Model for Coal Pyrolysis Optimization," Am. Chem. Soc., Div. Fuel Chem. Preprints, 20, No. 1 p. 161.

Rowe, P. N. [1971], in Fluidization, J. F. Davidson and D. Harrison, editors, Academic Press, London and New York, p. 121.

Salvador, L. A. and D. Keairns [1977a], "Advanced Coal Gasification System for Electric Power Generation Research and Development," Quarterly Progress Report, October 1976 - December 1976, Energy Research and Development Administration Report FE 1514-61.

Salvador, L. A. and D. Keairns [1977b], "Advanced Coal Gasification System for Electric Power Generation Research and Development," Quarterly Progress Report, April 1977 - June 1977, Energy Reserach and Development Administration Report FE 1514-69.

Schneyer, G. P., D. H. Brownell, Jr., W. D. Henline, and T. R. Blake [1978], " A Numerical Model of Coal Gasification in Entrained Flow Reactors," to be presented AIChE 71st Annual Meeting, Miami, Florida, November 1978.

Schroeder, W. C. [1962], to Fossil Fuels, Inc., "Hydrogenation of Coal," U. S. Patent 3,030,297, April 17, 1962.

Shapatina, E. A. V. A. Kalzuyhuyi, and Z. F. Chukhanov [1961], "Technological Utilization of Fuel for Energy, 1-Thermal Treatment of Fuels," (1960), BCURA Monthly Bulletin, 25, p. 285.

Smoot, L. D. and R. W. Hanks [1975], "The Influence of Mixing on Kinetic Processes in Entrained Coal Gasifiers," Quarterly Progress Report April 1975 - June 1975, Energy Research and Development Administration Report.

Stone, H. N., J. D. Batchelor, and H. F. Johnstone [1954], "Low Temperature Carbonization Rates in a Fluidized Bed," Ind. Eng. Chem. 46, p. 274.

Suuberg, E. M. [1977], Sc.D. Thesis, Massachusetts Institute of Technology.

Suuberg, E. M., W. A. Peters and J. B. Howard [1978], Ind. Eng. Chem. Process Design Dev., 17, p. 37.

Suuberg, E. M., W. A. Peters and J. B. Howard [1977], "Product Composition and Kinetics of Lignite Pyrolysis," Dept. of ChE, MIT, Cambridge, Massachusetts.

Van Krevelen, D. W. [1961], Coal, Elsevier Publishing Company, Amsterdam.

Van Krevelen, D. W., C. Van Heerden and F. J. Huntjens [1951], "Physiochemical Aspects of the Pyrolysis of Coal and Related Organic compounds," Fuel, 30, p. 253.

Wiser, W. H., G. R. Hill and N. J. Kertamus [1967], "Kinetic Study of the Pyrolysis of a High-Volatile Bituminous Coal," Ind. Eng. Chem. Process Design Dev., 6, p. 133.

☆U.S. GOVERNMENT PRINTING OFFICE: 1978-740-420/223